

Correlation between thermodynamical stabilities of metal borohydrides and cation electronegativities: First-principles calculations and experiments

Yuko Nakamori,¹ Kazutoshi Miwa,^{2,*} Akihito Ninomiya,¹ Haiwen Li,¹ Nobuko Ohba,² Shin-ichi Towata,² Andreas Züttel,^{3,4} and Shin-ichi Orimo^{1,†}

¹Institute for Materials Research, Tohoku University, Sendai 980-8577, Japan

²Toyota Central Research and Development Laboratories, Inc., Nagakute, Aichi 480-1192, Japan

³Physics Department, University of Fribourg, Perolles, Switzerland

⁴EMPA, Department of Environment, Energy and Mobility, Dübendorf, Switzerland

The thermodynamical stabilities for the series of metal borohydrides $M(\text{BH}_4)_n$ ($M=\text{Li, Na, K, Cu, Mg, Zn, Sc, Zr, and Hf}$; $n=1-4$) have been systematically investigated by first-principles calculations. The results indicated that an ionic bonding between M^{n+} cations and $[\text{BH}_4]^-$ anions exists in $M(\text{BH}_4)_n$, and the charge transfer from M^{n+} cations to $[\text{BH}_4]^-$ anions is a key feature for the stability of $M(\text{BH}_4)_n$. A good correlation between the heat of formation ΔH_{boro} of $M(\text{BH}_4)_n$ and the Pauling electronegativity of the cation χ_P can be found, which is represented by the linear relation, $\Delta H_{\text{boro}}=248.7\chi_P-390.8$ in the unit of kJ/mol BH_4 . In order to confirm the predicted correlation experimentally, the hydrogen desorption reactions were studied for $M(\text{BH}_4)_n$ ($M=\text{Li, Na, K, Mg, Zn, Sc, Zr, and Hf}$), where the samples of the later five borohydrides were mechanochemically synthesized. The thermal desorption analyses indicate that LiBH_4 , NaBH_4 , and KBH_4 desorb hydrogen to hydride phases. $\text{Mg}(\text{BH}_4)_2$, $\text{Sc}(\text{BH}_4)_3$, and $\text{Zr}(\text{BH}_4)_4$ show multistep desorption reactions through the intermediate phases of hydrides and/or borides. On the other hand, $\text{Zn}(\text{BH}_4)_2$ desorbs hydrogen and borane to elemental Zn due to instabilities of Zn hydride and boride. A correlation between the desorption temperature T_d and the Pauling electronegativity χ_P is observed experimentally and so χ_P is an indicator to approximately estimate the stability of $M(\text{BH}_4)_n$. The enthalpy change for the desorption reaction, ΔH_{des} , is estimated using the predicted ΔH_{boro} and the reported data for decomposed product, $\Delta H_{\text{hyd/boride}}$. The estimated ΔH_{des} show a good correlation with the observed T_d , indicating that the predicted stability of borohydride is experimentally supported. These results are useful for exploring $M(\text{BH}_4)_n$ with appropriate stability as hydrogen storage materials.

I. INTRODUCTION

Complex hydrides have attracted considerable attention as hydrogen storage materials, because of their high gravimetric hydrogen densities. Since Bogdanović and Schwickardi have reported that the catalyzed sodium alanate (NaAlH_4) shows reversible hydrogen desorption and absorption reactions at moderate condition,¹ many researches have been done for alkali complex hydrides mainly from the viewpoint of kinetics.²⁻¹⁰

Among alkali complex hydrides, lithium borohydride (LiBH_4) is one of the candidates for hydrogen storage materials because of its extremely high gravimetric hydrogen density (18 mass %). LiBH_4 mixed with SiO_2 has been reported to desorb hydrogen below 673 K that is lower than pure LiBH_4 does.¹¹ In order to decrease the hydrogen desorption temperatures, especially to 300–400 K, the systematic understanding of the thermodynamical stabilities is of great important. Recently, the stabilities of alkali borohydrides have been studied by first-principles calculation.¹²⁻¹⁶ Our calculated results for LiBH_4 revealed that the charge compensation by Li^+ is a key feature for the stability of the internal bonding of $[\text{BH}_4]^-$ anion¹² and it was expected that the suppression of the charge transfer by partial substitution of the element having larger electronegativity than Li is effective for lowering the hydrogen desorption temperature.¹⁷ In fact, Mg-substituted LiBH_4 has a lower thermal desorption temperature than pure LiBH_4 .¹⁸

In this study, the stabilities of not only alkali borohydrides but also other metal borohydrides are investigated to systematic understand of the thermodynamical stabilities of borohydrides. The heats of formation of borohydrides $M(\text{BH}_4)_n$, ($M=\text{Li, Na, K, Cu, Mg, Zn, Sc, Zr, and Hf}$, $n=1-4$; depending on valency) are predicted by first-principles calculations. And then, the thermal desorption temperatures are studied for $M(\text{BH}_4)_n$ ($M=\text{Li, Na, K, Mg, Zn, Sc, Zr, and Hf}$), where the samples of the later five borohydrides are mechanochemically synthesized.

In the theoretical prediction, the stabilities of metal borohydrides are discussed for the solid phase at the absolute zero temperature though some compounds show phase transitions below the hydrogen desorption temperature. Since the contribution of the latent heat for the phase transition to the energetics of the hydrogen desorption reaction is expected to be relatively modest,¹⁹ the predicted stabilities can be linked well to the experimental observations.

II. METHODS

A. Computational method

The present calculations were performed using the ultrasoft pseudopotential method²⁰ based on density functional theory.²¹ The generalized gradient approximation²² is adopted for the exchange-correlation energy. The cutoff energies used in this study are 15 and 120 hartrees for the

pseudowave functions and the charge density, respectively. The k -point grids for the Brillouin zone integration are generated so as to make the edge lengths of the grid elements as close to the target value of 0.08 bohr^{-1} as possible. These computational conditions give good convergence for the total energy within 1 meV/atom. The computational details can be found in Ref. 12 and the references therein.

B. Experimental procedure

LiBH_4 , NaBH_4 , and KBH_4 with 95–99.9 % purities were purchased from Aldrich Co. LTD. $M(\text{BH}_4)_n$ ($M=\text{Mg}$, Zn , Sc , Zr , and Hf) were synthesized by mechanical milling of the mixture of $M\text{Cl}_n$ and $n\text{LiBH}_4$ under 0.1 MPa argon atmosphere for 5 hours. Mechanochemical synthesis have been reported for preparation of $\text{Zn}(\text{BH}_4)_2$ (Ref. 23) and $\text{Zr}(\text{BH}_4)_4$.²⁴ The expected reaction during milling is expressed as follows:

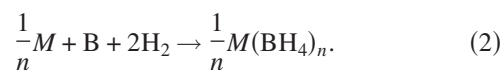


The samples thus prepared were examined by powder x-ray diffraction measurement (PANalytical X'PERT with Cu- $K\alpha$ radiation), Raman spectroscopy (Nicolet, Almega-HD, 532 nm laser with back scattering geometry) and thermal desorption spectroscopy detected by gas chromatography (GL Science GC323, argon flow rate of 40 ml/min and heating rate of 5 K/min). The samples were always handled in an argon glove box filled with purified argon (dew point below 183 K) without exposing air. The experimental details were described in Refs. 25 and 26.

III. RESULTS AND DISCUSSION

A. Theoretical predictions

We have predicted the heats of formation ΔH_{boro} for several borohydrides. Although most metal cations considered here form hydrides and/or borides, we restrict ourselves in this section to the heats of formation corresponding to the following reaction:



In order to compare the stability of borohydrides composed of the metal cations M which have different valency, we normalize ΔH_{boro} by the number of BH_4 complexes in the formula unit. The heat of formation is estimated from the difference of the total energies between the left- and right-hand sides of Eq. (2). The zero-point energies (ZPEs) are not taken into account, unless otherwise noted. The metal cation in the borohydride contributes mainly to the librational vibrations whose frequencies are thought to be considerably lower than those of the internal B-H bending and stretching modes of $[\text{BH}_4]^-$ anions.^{12,17} The phonon frequencies of the bulk metal are also expected to be low. Therefore, the ZPE contributions to ΔH_{boro} become nearly constant for the reaction shown in Eq. (2), regardless of metal cations. From the vibrational frequencies obtained for an isolated $[\text{BH}_4]^-$ anion and an H_2 molecule,¹² the amount of the ZPE correction is estimated to be 33 kJ/mol BH_4 . This estimation agrees well with the ZPE correction of 34 kJ/mol BH_4 for LiBH_4 .¹² We also confirm that this approximation is good for NaBH_4 as shown in the Appendix.

The predicted heats of formation without the ZPE correction for LiBH_4 and CuBH_4 are -194 and 43 kJ/mol BH_4 , respectively, which have been already presented in Refs. 12 and 17. The crystal structures of NaBH_4 and KBH_4 at ambient conditions are the NaCl type.²⁷ For NaBH_4 , we obtain the lattice constant as $a=6.137 \text{ \AA}$ which agrees well with the experimental values²⁸ of 6.12 \AA and the heat of formation as $\Delta H_{\text{boro}}=-182$ kJ/mol BH_4 . However, the phonon calculation gives a soft mode of $77i \text{ cm}^{-1}$ at the Γ point, indicating that the cubic NaCl-type structure is unstable at the zero temperature. This is most likely related to the phase transition to a tetragonal structure at low temperature. The recent structural analysis by neutron diffraction²⁹ shows that the tetragonal phase has $P4_2/nmc$ symmetry. We repeat the calculation for this phase and find the energy gain, $\Delta H_{\text{boro}}=-188$ kJ/mol BH_4 . For NaCl-type KBH_4 , the lattice constant and the heat of formation are predicted to be $a=6.739 \text{ \AA}$ and $\Delta H_{\text{boro}}=-228$ kJ/mol BH_4 , respectively. The agreement between the

TABLE I. Structural parameters of NaBH_4 and KBH_4 . The values in parentheses are the experimental data (Ref. 29 for NaBH_4 and Ref. 31 for KBH_4).

Compound	Space group	Lattice parameters (\AA)	Atom parameters				
			Position	x	y	z	
NaBH_4	$P4_2/nmc$ (No.137)	$a=4.339$	Na	$2a$	0	0	0
		($a=4.332$)	B	$2b$	0	0	1/2
		$c=5.949$	H	$8g$	0	0.2338	0.6179
		($c=5.869$)			(0.2307)	(0.6192)	
KBH_4	$P4_2/nmc$ (No.137)	$a=4.749$	K	$2a$	0	0	0
		($a=4.684$)	B	$2b$	0	0	1/2
		$c=6.662$	H	$8g$	0	0.2131	0.6072
		($c=6.571$)			(0.2100)	(0.6060)	

TABLE II. Structural parameters of Zr(BH₄)₄ and Hf(BH₄)₄.

Compound	Space group	Lattice parameters (Å)	Atom parameters				
			Position	x	y	z	
Zr(BH ₄) ₄	$P\bar{4}3m$ (No.215)	$a=5.795$	Zr	$1a$	0	0	0
			B	$4e$	0.2301	0.2301	0.2301
			H1	$4e$	0.3493	0.3493	0.3493
			H2	$12i$	0.2604	0.2604	0.0173
Hf(BH ₄) ₄	$P23$ (No.195)	$a=6.012$	Hf	$1a$	0	0	0
			B	$4e$	0.2204	0.2204	0.2204
			H1	$4e$	0.3355	0.3355	0.3355
			H2	$12j$	0.2710	0.2256	0.0171

calculated lattice constant and the measured one³⁰ (6.73 Å) is very good. Though no soft-mode instabilities are found for the cubic phase, it has been reported that KBH₄ also undergo a phase transition to the tetragonal structure with space group $P4_2/nmc$ at 70–65 K.³¹ The calculation for this phase gives small energy gain from the cubic phase, where the heat of formation is predicted as $\Delta H_{\text{boro}}=-231$ kJ/mol BH₄. The structural parameters of NaBH₄ and KBH₄ with $P4_2/nmc$ symmetry are given in Table I, which are in fairly good agreement with experimental data.^{29,31}

Table II indicates the optimized structural parameters for Zr(BH₄)₄ and Hf(BH₄)₄. The structure of Zr(BH₄)₄ is cubic with space group $P\bar{4}3m$.³² Four BH₄ complexes are tetrahedrally arranged around a Zr atom, where three of four hydrogen atoms in a BH₄ complex form bridging bonds with Zr. The optimized lattice constant is $a=5.795$ Å which agrees well with the experimental value³² of 5.86 Å. The heat of formation is predicted as $\Delta H_{\text{boro}}=-87$ kJ/mol BH₄. Hf(BH₄)₄ with $P\bar{4}3m$ symmetry has a soft mode of $155i$ cm⁻¹. The eigenvectors correspond to nearly rigid rotations of BH₄ complexes around Hf-B axes. Freezing this soft mode, the symmetry reduces to $P23$ for which $\Delta H_{\text{boro}}=-$

94 kJ/mol BH₄. Similar reduction of the symmetry has been reported for a Hf(BH₄)₄ molecule.³³

Although a synthesis of Mg(BH₄)₂ can be found in literature,³⁴ in our knowledge, no structural information is available. Since the effective ionic radius of a [BH₄]⁻ anion has been reported²⁷ as 2.03 Å which is close to the ionic radii of Br⁻ (1.96 Å) and I⁻ (2.20 Å), we refer the structures of Mg bromide and iodide to estimate the arrangement of cations and anions. The structure of MgBr₂ and MgI₂ is the CdI₂ type which has a trigonal basic block composed of I-Cd-I layers; iodide anions form two triangle nets and cations occupy the octahedral sites between them. The CdI₂ type structure contains four basic blocks. In order to determine the stable orientation of BH₄ complexes, the structural optimization is performed for the unit cells containing one trigonal basic block, assuming several high symmetry orientations for BH₄ complexes. The most stable structure found for this trigonal unit cell is given in Table III, where $\Delta H_{\text{boro}}=-99$ kJ/mol BH₄. Note that the cation-anion arrangement of Mg(AlH₄)₂ is the same as that of trigonal Mg(BH₄)₂, but the orientation of tetrahedral complex anions is different.³⁵ When we assume the same orientation for complex anions as Mg(AlH₄)₂, $\Delta H_{\text{boro}}=-59$ kJ/mol BH₄. Al-

TABLE III. Structural parameters of Mg(BH₄)₂.

Phase	Space group	Lattice parameters (Å)	Atom parameters				
			Position	x	y	z	
Trigonal	$P\bar{3}m_1$ (No.164)	$a=4.279$ $c=5.761$	Mg	$1a$	0	0	0
			B	$2d$	1/3	2/3	0.1877
			H1	$2d$	1/3	2/3	0.9752
			H2	$6i$	0.1792	-0.1792	0.2688
Monoclinic	$P2/c$ (No.13)	$a=6.777$ $b=5.552$ $c=8.085$ $\beta=75.40^\circ$	Mg	$2e$	1/4	0.9997	0
			B	$4g$	0.0583	0.8296	0.8051
			H1	$4g$	0.1040	0.8024	0.6524
			H2	$4g$	0.1840	0.7280	0.8705
			H3	$4g$	0.1064	0.2721	0.1289
			H4	$4g$	0.0495	0.0519	0.8348

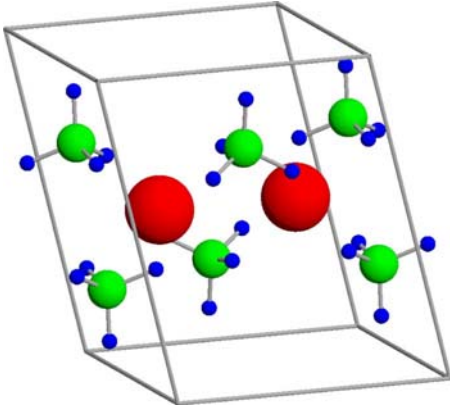


FIG. 1. (Color online) Crystal structure of monoclinic $\text{Mg}(\text{BH}_4)_2$. Red (large), green (middle), and blue (small) spheres represent Mg, B, and H atoms, respectively.

though we repeat the calculation for the CdI_2 -type structure using the obtained BH_4 orientation, the heat of formation is hardly changed from that of the trigonal basic unit cell, indicating that the stacking of the basic blocks has only minor effects. Some of the trigonal basic unit cells have strong instability with the soft modes of $630i-150i \text{ cm}^{-1}$, depending on the BH_4 orientations assumed. We investigate these instability using the extended unit cells up to 2×2 in the lateral direction, from which the stable monoclinic structure is found with $\Delta H_{\text{boro}} = -104 \text{ kJ/mol BH}_4$. Figure 1 shows the crystal structure of monoclinic $\text{Mg}(\text{BH}_4)_2$, the structural parameters of which are given in Table III. This heat of formation is the lowest value among the structures considered in this study. For examples, we also consider the structures of Zn bromide and iodide, since the ionic radius of Zn^{2+} is close to that of Mg^{2+} . The structure of ZnI_2 is the CdCl_2 type, which has the same trigonal basic block as the CdI_2 -type structure but the stacking of the blocks is different. The predicted heat of formation for CdCl_2 -type $\text{Mg}(\text{BH}_4)_2$ is -99 kJ/mol BH_4 which is essentially the same as that of the trigonal basic unit cell. The HgI_2 type is also the layer struc-

ture; anions form two square nets and cations sit in the tetrahedral sites between them. Trying several BH_4 orientations, we obtain $\Delta H_{\text{boro}} = -94 \text{ kJ/mol BH}_4$ for HgI_2 -type $\text{Mg}(\text{BH}_4)_2$. Because our structural survey may be still limited, in a strict sense, the heat of formation predicted for the monoclinic phase, $\Delta H_{\text{boro}} = -104 \text{ kJ/mol BH}_4$, gives only the upper bound for $\text{Mg}(\text{BH}_4)_2$. However, the heats of formation obtained for several prototypical structures are within the range of 10 kJ/mol BH_4 when the optimum BH_4 orientations are chosen. This implies that ΔH_{boro} is not affected strongly by the cation-anion arrangements. We expect that, even if the more stable structure exists, its heat of formation is not so far away from our prediction.

The structure of $\text{Zn}(\text{BH}_4)_2$ is also undetermined and so we have performed the courses of the structural survey as done for $\text{Mg}(\text{BH}_4)_2$. The most stable structure is predicted to be triclinic with $\Delta H_{\text{boro}} = -18 \text{ kJ/mol BH}_4$, whose structural parameters are given in Table IV. This structure is basically the same as that of monoclinic $\text{Mg}(\text{BH}_4)_2$. When the monoclinic symmetry is assumed for $\text{Zn}(\text{BH}_4)_2$, the weak instability with a soft mode of $20i \text{ cm}^{-1}$ appears. Trends that $\text{Zn}(\text{BH}_4)_2$ prefers lower symmetry than $\text{Mg}(\text{BH}_4)_2$ are also found for other prototypical structures. The optimized structures starting from the trigonal basic unit cell and the HgI_2 -type structure also become triclinic, for which the heats of formation are obtained as -7 and -6 kJ/mol BH_4 , respectively.

For $\text{Sc}(\text{BH}_4)_3$, the cation-anion arrangement is assumed to be the BiI_3 -type (Pearson symbol, $hR8$) with space group $R\bar{3}$. This is a simplified structure for ScBr_3 which has the $hR24$ structure with $R\bar{3}$ symmetry. The BiI_3 -type structure consists of the trigonal basic block similar to that of the CdI_2 type; anions form two triangle nets and cations occupy $2/3$ of the octahedral sites between them. The structural optimization gives a puckered configuration for the cation layers and tilted orientations for BH_4 complexes. The structural parameters of BiI_3 -type $\text{Sc}(\text{BH}_4)_3$ are listed in Table V and the corresponding atomic configuration for the trigonal basic block is shown in Fig. 2, where $\Delta H_{\text{boro}} = -105 \text{ kJ/mol BH}_4$.

TABLE IV. Structural parameters of triclinic $\text{Zn}(\text{BH}_4)_2$.

Space group	Lattice parameters (Å)	Atom parameters				
		Position	x	y	z	
$P\bar{1}$ (No.2)	$a=6.877$	Zn	$2i$	0.2498	0.0001	0.9998
	$b=5.440$	B1	$2i$	0.0567	0.8903	0.7939
	$c=7.842$	B2	$2i$	0.5497	0.1754	0.8166
	$\alpha=89.50^\circ$	H1	$2i$	0.0997	0.8534	0.6382
	$\beta=76.15^\circ$	H2	$2i$	0.5892	0.2640	0.6710
	$\gamma=89.98^\circ$	H3	$2i$	0.1789	0.7718	0.8612
		H4	$2i$	0.3316	0.7331	0.0999
		H5	$2i$	0.1031	0.2267	0.1397
	H6	$2i$	0.3863	0.2679	0.9011	
	H7	$2i$	0.0498	0.1135	0.8210	
	H8	$2i$	0.4481	0.0506	0.1928	

TABLE V. Structural parameters of BiI₃-type Sc(BH₄)₃.

Space group	Lattice parameters (Å)	Atom parameters				
		Position	<i>x</i>	<i>y</i>	<i>z</i>	
<i>R</i> $\bar{3}$ (No.148)	<i>a</i> =7.262	Sc	6 <i>c</i>	0	0	0.3210
	<i>c</i> =18.194	B	18 <i>f</i>	0.3503	0.3123	0.4079
		H1	18 <i>f</i>	0.4002	0.3671	0.3423
		H2	18 <i>f</i>	0.3691	0.4611	0.4432
		H3	18 <i>f</i>	0.1636	0.1647	0.4130
		H4	18 <i>f</i>	0.4588	0.2370	0.4329

In order to check the effect of the stacking of the trigonal basic blocks, the calculation is performed for the trigonal unit cell where the single block is repeated along the *c* axis. The heat of formation obtained is slightly higher than that of the BiI₃ type but the difference is less than 1 kJ/mol BH₄. We confirm that the stacking of the blocks is less important.

Figure 3 depicts the densities of states for borohydrides described above. The electronic structures are nonmetallic with relatively large energy gaps of 2.9–6.8 eV. The occupied states mainly consist of B-*sp*³ hybrids and H-1*s* orbitals. The contribution of metal atoms to the valence states are little except for the filled 3*d* states found in CuBH₄ and Zn(BH₄)₂. These figures support an ionic picture for the interaction between metal cations and [BH₄][−] anions.

As mentioned in Refs. 12 and 17, the charge transfer from metal cations to [BH₄][−] anions is expected to be a key feature for the stability of borohydrides. The ability of the charge transfer can be measured by the electronegativity, though the definition of the electronegativity is not unique and some formulations have been proposed.^{36–38} In this study, we use the Pauling scaling.³⁶ Since the formulation of the Pauling electronegativity is based on the difference of binding energies between the elements, it will be suitable for the present purpose. In Fig. 4, the heat of formation, ΔH_{boro} , as a function of the Pauling electronegativity of the cation, χ_P , is plotted, where the ZPE contributions to ΔH_{boro} are approximately taken into consideration by adding the correction of 33 kJ/mol BH₄ estimated from the results for an isolated [BH₄][−] anion and an H₂ molecule. A good correlation between ΔH_{boro} and χ_P can be found. Assuming the linear relation, the least square fitting yields

$$\Delta H_{\text{boro}} = 248.7\chi_P - 390.8, \quad (3)$$

with an absolute mean error of 10.4 kJ/mol BH₄. The Pauling electronegativity is a good indicator to estimate thermo-

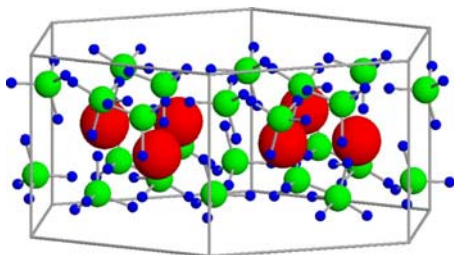


FIG. 2. (Color online) Atomic configuration for the trigonal basic block in BiI₃-type Sc(BH₄)₃. Red (large), green (middle), and blue (small) spheres represent Sc, B, and H atoms, respectively. The BiI₃-type Sc(BH₄)₃ consists of three blocks along the *c* axis with ABC stacking.

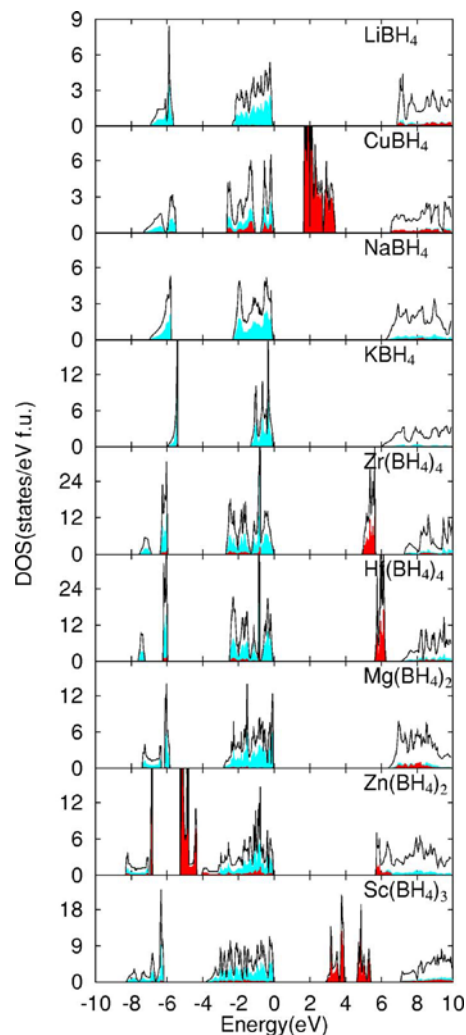


FIG. 3. (Color online) Total and partial densities of states (DOS) for borohydrides. The shaded-light (blue) parts indicate the partial DOS of boron and hydrogen atoms, and the shaded-dark (red) parts show the partial DOS of metal atoms. The origins of the energies are set to be the top of valence states except for CuBH₄, where the energy is shifted by +3.5 eV for clear comparison.

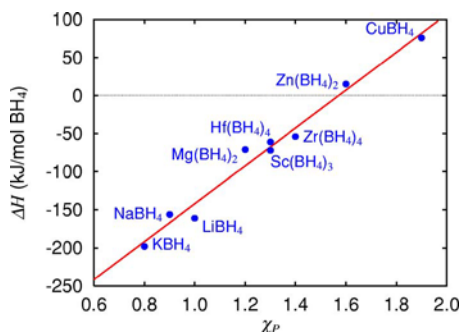


FIG. 4. (Color online) Relation between the heats of formation ΔH_{boro} and the Pauling electronegativities of cations, χ_P . The straight line indicates the result of the least square fitting, $\Delta H_{\text{boro}} = 248.7\chi_P - 390.8$. The zero-point energy contributions to ΔH_{boro} are approximately taken into consideration (see the text).

dynamical stability of borohydrides. From this relation, it is expected that borohydrides with $\chi_P \geq 1.6$ are thermodynamically unstable.

We also investigate the Mulliken scaling, χ_M .^{37,39} The correlation between ΔH_{boro} and χ_M is fairly good except for CuBH_4 . The calculated data excluding CuBH_4 can be fitted with an absolute mean error of 13.1 kJ/mol BH_4 . However, because the Mulliken electronegativities for Cu (4.48 eV) and Zn (4.45 eV) are almost the same, the difference of ΔH_{boro} between CuBH_4 and $\text{Zn}(\text{BH}_4)_2$ can not be explained by χ_M .

B. Experimental support

Based on the theoretical prediction in the preceding section, we have conducted the experiment to investigate the stabilities of borohydrides. Figure 5 shows the powder x-ray diffraction profiles of borohydrides. There are broad diffraction peaks at around 20 degree in all the profiles, originating from the diffraction of tape covering the samples to avoid (hydro-)oxidation by exposing air. The diffraction profile of LiBH_4 is well identified as a single phase of orthorhombic structure at room temperature. Because the heat of formation for CuBH_4 is a large positive value, CuBH_4 could not be synthesized at room temperature.⁴⁰ NaBH_4 , and KBH_4 crystallize in cubic symmetry with lattice constants of 6.163 and 6.727 Å, respectively, which are in good agreement with the theoretical prediction. $\text{Mg}(\text{BH}_4)_2$, $\text{Zn}(\text{BH}_4)_2$, $\text{Sc}(\text{BH}_4)_3$, $\text{Zr}(\text{BH}_4)_4$, and $\text{Hf}(\text{BH}_4)_4$ are mechanochemically synthesized according to Eq. (1). All the diffraction peaks after mechanical milling are identified as LiCl , although the diffraction peaks of LiCl after the milling of MgCl_2 and 2LiBH_4 shift to lower angle, probably due to partial substitution of Mg for Li in LiCl . It should be noted that there are no diffraction peaks of the starting materials of MCl_n and LiBH_4 , showing the progression of reaction of Eq. (1). However, there are no diffraction peaks of $\text{M}(\text{BH}_4)_n$ even though after annealing. This is most likely due to disordering of the crystal structure. We have reported that diffraction peaks became unclear and only small peaks were observed for rehydrogenated LiBH_4 , while the atomic vibrating modes of BH_4 anions in LiBH_4 were obviously detected.^{18,41} Therefore, we investigate the

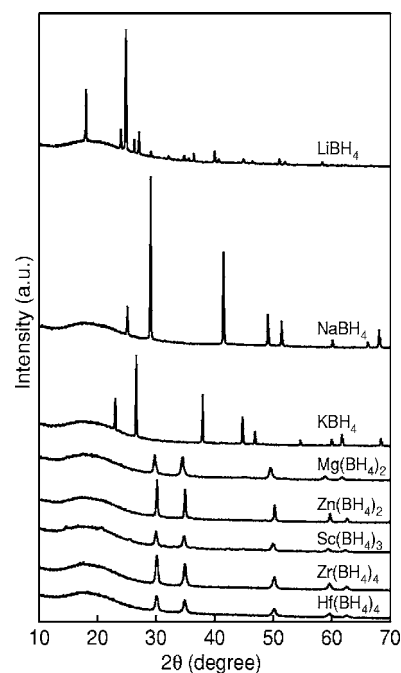


FIG. 5. Powder x-ray diffraction profiles of purchased MBH_4 ($M=\text{Li}$, Na , and K), and prepared $\text{M}(\text{BH}_4)_n$ ($M=\text{Mg}$, Zn , Sc , Zr , and Hf) by mechanical milling.

atomistic vibrations in order to confirm the existence of $\text{M}(\text{BH}_4)_n$.

Figure 6 shows the Raman spectra of the purchased MBH_4 ($M=\text{Li}$, Na , and K), and mechanochemically prepared $\text{M}(\text{BH}_4)_n$ ($M=\text{Mg}$, Zn , Sc , Zr , and Hf). Raman shift for LiBH_4 , NaBH_4 , and KBH_4 are observed at around 1300 and 2300 cm^{-1} , corresponding to the bending (ν_2 , and also ν'_2 only for LiBH_4) and stretching (ν_1) modes of B-H in

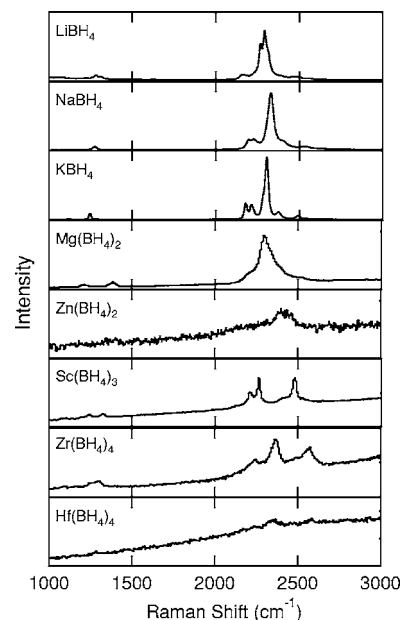


FIG. 6. Raman spectra of purchased MBH_4 ($M=\text{Li}$, Na , and K), and prepared $\text{M}(\text{BH}_4)_n$ ($M=\text{Mg}$, Zn , Sc , Zr , and Hf) by mechanical milling.

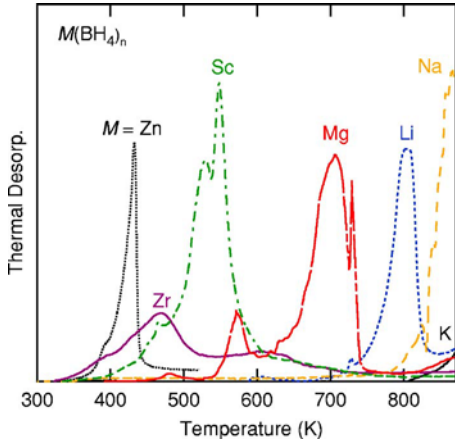


FIG. 7. (Color online) Thermal desorption profiles of $M(\text{BH}_4)_n$.

BH_4 anion.⁴² There are two bending and a stretching modes at around 1210, 1390, and 2300 cm^{-1} in the spectra of $\text{Mg}(\text{BH}_4)_2$, which are consistent with the IR spectra.⁴³ The measurement of Raman spectroscopy for $\text{Zn}(\text{BH}_4)_2$ was very difficult, because the sample was charred by laser irradiation. A small peak at around 2450 cm^{-1} was barely observed when the irradiation time is as short as one second. There are three and four Raman shifts at around 1200–1400 and 2100–2600 cm^{-1} in the spectra of $\text{Sc}(\text{BH}_4)_3$, which are expected to be bending and stretching of B-H vibrating modes. At the same wave number of 1310 and 2250–2580 cm^{-1} , bending and three stretching modes are observed for $\text{Zr}(\text{BH}_4)_4$ and $\text{Hf}(\text{BH}_4)_4$, which agrees roughly with the results in Refs. 44 and 33. The observed Raman modes are originated from the bending and stretching atomic vibrations in BH_4 anion, and the modes of $M(\text{BH}_4)_n$ ($M=\text{Mg}, \text{Zn}, \text{Sc}, \text{Zr},$ and Hf) are not the same as starting materials. We confirm LiCl and $M(\text{BH}_4)_n$ in the sample after mechanical milling as products of Eq. (1) by x-ray diffraction measurement and Raman spectroscopy, respectively.

The hydrogen desorption reactions accompanying the phase decomposition were studied by thermal desorption analysis as shown in Fig. 7. Although, the prepared $M(\text{BH}_4)_n$ for $M=\text{Mg}, \text{Zn}, \text{Sc}, \text{Zr},$ and Hf contain LiCl , the thermal desorption profiles are originating from $M(\text{BH}_4)_n$ only, because LiCl decomposes at higher temperature than its melting temperature of 878 K. $M\text{BH}_4$ for $M=\text{Li}, \text{Na},$ and K desorb hydrogen at higher temperature than 700 K, in which alkali hydrides remain up to 873 K.²⁵ There are multi-step desorption peaks of $M(\text{BH}_4)_n$ for $M=\text{Mg}, \text{Sc},$ and Zr , which suggest that the hydrogen desorption reactions from borohydride to hydride, and then from hydride to element and/or boride as was reported in $\text{Mg}(\text{BH}_4)_2$.^{43,45} There is a single desorption peak in $\text{Zn}(\text{BH}_4)_2$ because it decomposes directly to elemental Zn due to instabilities of Zn hydride and boride. The decomposition reaction of $\text{Hf}(\text{BH}_4)_4$ can not be studied because its boiling temperature of 391 K, that is lower than the decomposition temperature.⁴⁶

Here, the desorption temperature T_d is defined as a temperature of the first peak. In Fig. 8, T_d are plotted as a function of the Pauling electronegativity χ_P . A good correlation

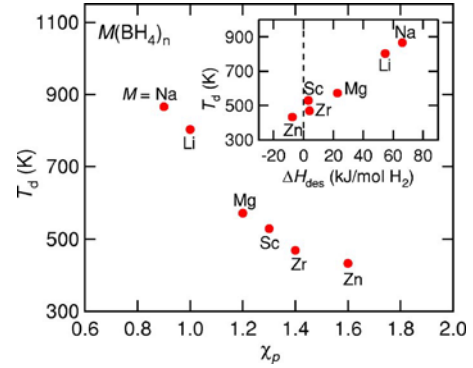
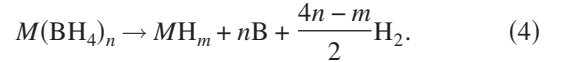


FIG. 8. (Color online) The desorption temperature T_d as a function of the Pauling electronegativity χ_P . Inset shows the correlation between T_d and estimated ΔH_{des} for the desorption reaction of Eq. (4).

between the desorption temperature T_d and the Pauling electronegativity χ_P is also observed experimentally, indicated that T_d can be approximately estimated by considering χ_P as an indicator.

Since the desorption reactions are accompanied with the formation of hydrides and/or borides except for $\text{Zn}(\text{BH}_4)_2$ as mentioned above, the stability of decomposed products has to be taken into account. We assume that the borohydrides except for $\text{Zn}(\text{BH}_4)_2$ decompose to hydrides in the first desorption reaction as follow:⁴⁷



The enthalpy change for this reaction, ΔH_{des} , can be estimated using the predicted ΔH_{boro} for $M(\text{BH}_4)_n$ and the experimental data for $M\text{H}_m$, ΔH_{hyd} .^{48–50} The relation between estimated ΔH_{des} for the desorption reaction of Eq. (4) and the observed T_d is shown in the inset of Fig. 8. There is also a good correlation between ΔH_{des} and T_d , indicating that the predicted stabilities of borohydrides are experimentally supported. Because the thermodynamical stabilities were well investigated for binary hydrides and borides, one can easily deduce ΔH_{des} using Eq. (3) for $M(\text{BH}_4)_n$ and the reported data for binary hydrides and borides.

We detect by mass spectroscopy that the components of desorbed gas from $M(\text{BH}_4)_n$ for $M=\text{Li}, \text{Na}, \text{K}, \text{Mg}, \text{Sc},$ and Zr ($\chi_P \leq 1.4$) are only hydrogen, while $\text{Zn}(\text{BH}_4)_2$ ($\chi_P=1.6$) desorbs also borane^{51,52} which might be related to the thermodynamical instability predicted. On the other hand, $M\text{BH}_4$ for $M=\text{Li}, \text{Na},$ and K ($\chi_P \leq 1.0$) are too stable, and their T_d are high. The suitable χ_P in $M(\text{BH}_4)_n$ for hydrogen storage is expected to be between them, approximately 1.2–1.5.

The observed T_d are related to also kinetics, that may require higher temperatures than those predicted from the thermodynamical stabilities to promote desorption reactions. In order to precisely evaluate ΔH_{des} for the desorption reaction of $M(\text{BH}_4)_n$ experimentally, the measurement of pressure composition isotherm is in progress.

IV. SUMMARY

The thermodynamical stabilities of metal borohydrides, $M(\text{BH}_4)_n$ ($M=\text{Li}, \text{Na}, \text{K}, \text{Cu}, \text{Mg}, \text{Zn}, \text{Sc}, \text{Zr},$ and Hf ,

$n=1-4$) have been systematically investigated by first-principles calculations. In the cases of $M=\text{Mg}$, Zn , and Sc , for which no structural information is available, the crystal structures are modeled by referring those of bromides and iodides, since the effective ionic radius of $[\text{BH}_4]^-$ is close to the ionic radii of Br^- and I^- . The electronic structures are found to be nonmetallic for all borohydrides considered in this study. The heats of formation normalized by the number of BH_4 complexes, ΔH_{boro} , show a good correlation with the Pauling electronegativities of cations, χ_P , which is represented by the linear relation, $\Delta H_{\text{boro}}=248.7\chi_P-390.8$ in the unit of kJ/mol BH_4 .

In order to investigate the thermal desorption temperatures experimentally, $M(\text{BH}_4)_n$ ($M=\text{Mg}$, Zn , Sc , Zr , and Hf) were mechanochemically synthesized by milling of the mixture of $M\text{Cl}_n$ and LiBH_4 . After mechanical milling, formations of LiCl and $M(\text{BH}_4)_n$ are confirmed by x-ray diffraction measurement and Raman spectroscopy, respectively. The thermal desorption analyses are performed up to 873 K, and the results indicate that LiBH_4 , NaBH_4 , and KBH_4 desorb hydrogen to hydride phases. $\text{Mg}(\text{BH}_4)_2$, $\text{Sc}(\text{BH}_4)_3$, and $\text{Zr}(\text{BH}_4)_4$ show multistep desorption reactions through the intermediate phases of hydrides and/or borides. On the other hand, $\text{Zn}(\text{BH}_4)_2$ desorbs hydrogen to elemental Zn due to instabilities of Zn hydride and boride, although desorbed gas contains also borane. A good correlation between the desorption temperature T_d and χ_P is observed experimentally and so χ_P is an indicator to approximately estimate the stability of $M(\text{BH}_4)_n$. The estimated ΔH_{des} for the desorption reaction show a good correlation with T_d . Therefore, ΔH_{des} as an indicator for exploring useful hydrogen storage materials with appropriate stability, can be estimated using ΔH_{boro} for $M(\text{BH}_4)_n$ predicted in this study and $\Delta H_{\text{hyd/boride}}$ reported extensively.

ACKNOWLEDGMENTS

The authors would like to thank T. Noritake, M. Aoki, and S. Hyodo for valuable discussions, and N. Warifune for technical support. This study was partially supported by the New Energy and Industrial Technology Development Organization (NEDO), International Joint Research under the ‘‘Development for Safe Utilization and Infrastructure of hydrogen’’ Project (2005–2006), and by the Ministry of Education, Science, Sports and Culture, Grant-in-Aid for Encouragement of Young Scientists (B), Grant No. 17760555 and for Scientific Research (A), Grant No. 18206073.

APPENDIX

In this appendix, we calculate the ZPE contribution to the heat of formation for tetragonal NaBH_4 with $P4_2/nmc$ symmetry in order to examine approximate treatment for the ZPE correction described in Sec. III A. The zero-point energies are obtained within the harmonic approximation and the phonon eigenmodes are calculated by the force-constant method.⁵³ For bcc-Na, the zero-point energy is predicted as 16 meV/atom, where the supercell containing 64 atoms with the theoretical lattice constant of $a=4.184 \text{ \AA}$ are used. The

TABLE VI. Dielectric properties of tetragonal NaBH_4 . Macroscopic high-frequency dielectric permittivity tensors ϵ_∞ and Born effective charge tensor Z^* . The yy element is the same as xx , and $|Z_{xy}^*|=|Z_{yx}^*|$, $|Z_{yz}^*|=|Z_{zy}^*|$, and $|Z_{zx}^*|=|Z_{xz}^*|$ for Z_{H}^* .

	xx	zz	xy	yz	zx
ϵ_∞	2.56	2.50	0	0	0
Z_{Na}^*	1.14	1.16	0	0	0
Z_{B}^*	0.20	0.17	0	0	0
Z_{H}^*	-0.34	-0.33	± 0.15	± 0.16	± 0.14

zero-point energies are 126 and 135 meV/atom for $\alpha\text{-B}$ and H_2 , respectively.¹²

The zero-point energy for NaBH_4 is estimated from only the Γ -phonon eigenmodes as done for LiBH_4 .¹² Since the tetragonal unit cell contains two formula units, there are 33 optical Γ -phonon modes. The irreducible representation of them is $2A_{1g}+A_{2g}+B_{1g}+4B_{2g}+5E_g+A_{1u}+3A_{2u}+2B_{1u}+B_{2u}+4E_u$; *gerade* modes except for A_{2g} are Raman active, A_{2u} and E_u modes are infrared active, and others are inactive. The infrared active modes are divided into the transverse optical (TO) modes and the longitudinal optical (LO) modes. Knowledge of the dielectric properties is required to treat this splitting. Table VI summarizes the dielectric properties, which are obtained using the linear response calculation.^{54,55} These values are quite similar to those of LiBH_4 . The Γ -phonon frequencies of tetragonal NaBH_4 are listed in Table VII, from which the zero-point energy is obtained as 172 meV/atom. The eigenmodes around 1100–1300 and 2300–2400 cm^{-1} originate from the internal B-H bending and stretching vibrations of BH_4 complexes. These frequencies are in good agreement with the Raman spectroscopy measurements given in Sec. III B.

Using the zero-point energies obtained in this Appendix, the ZPE correction to ΔH_{boro} is predicted to be 34 kJ/mol BH_4 for tetragonal NaBH_4 . This is in good agreement with the estimated value of 33 kJ/mol BH_4 . This supports approximate treatment for the ZPE correction adopted in Sec. III A.

TABLE VII. Optical Γ -phonon frequencies (cm^{-1}) of tetragonal NaBH_4 .

Modes	Frequencies				
A_{1g}	1241	2323			
A_{2g}	353				
B_{1g}	1231				
B_{2g}	132	238	1104	2380	
E_g	95	140	333	1091	2345
A_{1u}	1220				
A_{2u} (TO)	177	1097	2343		
A_{2u} (LO)	283	1106	2380		
B_{1u}	1240	2317			
B_{2u}	170				
E_u (TO)	137	231	1079	2316	
E_u (LO)	227	258	1089	2350	

*Electronic address: miwa@cmp.tytlabs.co.jp

†Electronic address: orimo@imr.tohoku.ac.jp

- ¹B. Bogdanović and M. Schwickardi, *J. Alloys Compd.* **253**, 1 (1997).
- ²R. A. Zidan, S. Takara, A. G. Hee, and C. M. Jensen, *J. Alloys Compd.* **285**, 119 (1999).
- ³L. Zaluski, A. Zaluska, and J. O. Ström-Olsen, *J. Alloys Compd.* **290**, 71 (1999).
- ⁴K. J. Gross, S. Guthrie, S. Takara, and G. Thomas, *J. Alloys Compd.* **297**, 270 (2000).
- ⁵B. Bogdanović, R. A. Brand, A. Marjanović, M. Schwickardi, and J. Tölle, *J. Alloys Compd.* **302**, 36 (2000).
- ⁶C. M. Jensen and K. J. Gross, *Appl. Phys. A: Mater. Sci. Process.* **71**, 213 (2001).
- ⁷D. Sun, T. Kiyobayashi, H. Takeshita, N. Kuriyama, and C. M. Jensen, *J. Alloys Compd.* **337**, L8 (2002).
- ⁸G. P. Meisner, G. G. Tibbetts, F. E. Pinkerton, C. H. Olk, and M. P. Balogh, *J. Alloys Compd.* **337**, 254 (2002).
- ⁹G. Sandrock, K. Gross, and G. Thomas, *J. Alloys Compd.* **339**, 299 (2002).
- ¹⁰H. Morioka, K. Kakizaki, S. C. Chung, and A. Yamada, *J. Alloys Compd.* **353**, 310 (2003).
- ¹¹A. Züttel, P. Wenger, S. Rentsch, P. Sudan, Ph. Mauron, and Ch. Emmenegger, *J. Power Sources* **118**, 1 (2003).
- ¹²K. Miwa, N. Ohba, S. Towata, Y. Nakamori, and S. Orimo, *Phys. Rev. B* **69**, 245120 (2004).
- ¹³M. E. Arroyo and G. Ceder, *J. Alloys Compd.* **364**, 6 (2004).
- ¹⁴Z. Lodziana and T. Vegge, *Phys. Rev. Lett.* **93**, 145501 (2004).
- ¹⁵P. Vajeeston, P. Ravindran, A. Kjekshus, and H. Fjellvåg, *J. Alloys Compd.* **387**, 97 (2005).
- ¹⁶N. Ohba, K. Miwa, M. Aoki, T. Noritake, S. Towata, Y. Nakamori, S. Orimo, and A. Züttel, cond-mat/0606228 (unpublished).
- ¹⁷K. Miwa, N. Ohba, S. Towata, Y. Nakamori, and S. Orimo, *J. Alloys Compd.* **404-406**, 140 (2005).
- ¹⁸S. Orimo, Y. Nakamori, G. Kitahara, K. Miwa, N. Ohba, S. Towata, and A. Züttel, *J. Alloys Compd.* **404-406**, 427 (2005).
- ¹⁹For LiBH₄, the latent heats for structural change at 381 K and fusion at 540 K has been reported as 4.2 and 7.6 kJ/mol, respectively; M. B. Smith and G. E. Bass Jr., *J. Chem. Eng. Data* **8**, 342 (1963).
- ²⁰D. Vanderbilt, *Phys. Rev. B* **41**, R7892 (1990); K. Laasonen, A. Pasquarello, R. Car, C. Lee, and D. Vanderbilt, *ibid.* **47**, 10142 (1993).
- ²¹P. Hohenberg and W. Kohn, *Phys. Rev.* **136**, B864 (1964); W. Kohn and L. J. Sham, *Phys. Rev.* **140**, A1133 (1965).
- ²²J. P. Perdew, K. Burke, and M. Ernzerhof, *Phys. Rev. Lett.* **77**, 3865 (1996); **78**, 1396 (1997).
- ²³V. E. Wiberger and W. Henle, *Z. Naturforsch. B* **7b**, 579 (1952).
- ²⁴V. V. Volkov, K. G. Myakishev, and S. I. Yugov, *J. Appl. Chem. USSR* **48**, 2184 (1975).
- ²⁵S. Orimo, Y. Nakamori, and A. Züttel, *Mater. Sci. Eng., B* **108**, 51 (2003).
- ²⁶Y. Nakamori, A. Ninomiya, G. Kitahara, M. Aoki, T. Noritake, K. Miwa, Y. Kojima, and S. Orimo, *J. Power Sources* **155**, 447 (2006).
- ²⁷C. W. F. T. Pistorius, *Z. Phys. Chem., Neue Folge* **88**, 253 (1974).
- ²⁸A. M. Soldate, *J. Am. Chem. Soc.* **69**, 987 (1947).
- ²⁹P. Fischer and A. Züttel, *Mater. Sci. Forum* **443-444**, 287 (2004).
- ³⁰S. C. Abrahams and K. Kalnajs, *J. Chem. Phys.* **22**, 434 (1954).
- ³¹G. Renaudin, S. Gomes, H. Hagemann, L. Keller, and K. Yvon, *J. Alloys Compd.* **375**, 98 (2004).
- ³²P. H. Bird and M. R. Churchill, *Chem. Commun. (London)* **1967**, 403 (1967).
- ³³J. O. Jensen, *Spectrochim. Acta, Part A* **59**, 379 (1993).
- ³⁴E. A. Sullivan and R. C. Wade, *Gravity Concentration to Hydrogen Energy*, Kirk-Othmer Encyclopedia of Chem. Tech. Vol. 12, 3rd ed. (Wiley-Interscience, New York, 1980), p. 772.
- ³⁵M. Fichtner, J. Engel, O. Fuhr, A. Glöss, O. Rubner, and R. Ahlrichs, *Inorg. Chem.* **42**, 7060 (2003).
- ³⁶L. Pauling, *The Nature of the Chemical Bonds*, 3rd ed. (Cornell University Press, New York, 1960).
- ³⁷R. S. Mulliken, *Chem. Phys.* **2**, 783 (1934).
- ³⁸A. L. Allred and E. G. Rochow, *J. Inorg. Nucl. Chem.* **5**, 264 (1958).
- ³⁹R. G. Parr and R. G. Pearson, *J. Am. Chem. Soc.* **105**, 7512 (1983).
- ⁴⁰T. J. Kligen, *Inorg. Chem.* **3**, 1058 (1964).
- ⁴¹Our preliminary measurement of pressure-composition isotherm for LiBH₄ indicated that ΔH was not affected by disordering of the crystal structure. The thermal desorption profile with disordering of the crystal structure was similar to that without disordering as shown in Ref. 18. The observed disordering of the crystal structure made a very small impact on T_d .
- ⁴²J.-Ph. Soulié, G. Renaudin, R. Eerný, and K. Yvon, *J. Alloys Compd.* **346**, 200 (2002).
- ⁴³V. N. Konoplev and V. M. Bakulina, *Izv. Akad. Nauk. SSR, Ser. Khi.* **1**, 159 (1971).
- ⁴⁴N. Davies, M. G. H. Wallbridge, B. E. Smith, and B. D. James, *J. Chem. Soc. Dalton Trans.* **1977**, 710.
- ⁴⁵T. Matsunaga, F. Buchter, K. Miwa, S. Towata, S. Orimo, and A. Züttel (unpublished).
- ⁴⁶H. R. Hoekstra and J. J. Katz, *J. Am. Chem. Soc.* **71**, 2488 (1949).
- ⁴⁷The decomposed products for $M=\text{Sc}$ and Zr could not be clarified, because only LiCl was observed experimentally in the x-ray diffraction profile after desorption reactions.
- ⁴⁸The used ΔH_{hyd} of MH_m are -118, -114, -158, -74, -200, and -188 kJ/mol H₂ for KH, NaH, LiH, MgH₂, ScH₂, and ZrH₂, respectively. Since Zn hydride is unstable, ΔH_{des} of Zn(BH₄)₂ was deduced from Eq. (2) assuming that only hydrogen is desorbed.
- ⁴⁹<http://hydropark.ca.sandia.gov/MaterialsFrame2.html>
- ⁵⁰*Phase Diagrams of Binary Hydrogen Alloys*, edited by F. D. Manchester (ASM International, 2000).
- ⁵¹The components of desorbed gas and mechanochemically synthesis for Zn(BH₄)₂ have been also reported by Jeon and Cho recently; E. Jeon and Y. W. Cho, *J. Alloys Compd.* (to be published).
- ⁵²Y. Nakamori, H.-W. Li, K. Miwa, S. Towata, and S. Orimo, *Mater. Trans.* (to be published).
- ⁵³K. Kunc and R. M. Martin, *Phys. Rev. Lett.* **48**, 406 (1982).
- ⁵⁴X. Gonze and C. Lee, *Phys. Rev. B* **55**, 10355 (1997).
- ⁵⁵N. Ohba, K. Miwa, N. Nagasako, and A. Fukumoto, *Phys. Rev. B* **63**, 115207 (2001).